

Electronic Supplementary Information (ESI)

## Effect of linear and non-linear pseudohalides on structural and magnetic properties of Co(II) hexacoordinate single-molecule magnets

L. Váhovská,<sup>a,b</sup> S. Vitushkina,<sup>c</sup> I. Potočnák,<sup>b</sup> Z. Trávníček<sup>d</sup> and R. Herchel<sup>\*d</sup>

<sup>a</sup>P. J. Šafarik University in Košice, Department of Inorganic Chemistry, Institute of Chemistry, Moyzesova 11, Košice, Slovakia.

<sup>b</sup>University of Veterinary Medicine and Pharmacy in Košice, Department of Chemistry, Biochemistry and Biophysics, Institute of Biochemistry, Komenského 73, Košice, Slovakia.

<sup>c</sup>V.N. Karazin Kharkov National University, Faculty of Chemistry, Department of Applied Chemistry, Svobody sq. 4, Kharkov, Ukraine.

<sup>d</sup>Department of Inorganic Chemistry, Regional Centre of Advanced Technologies and Materials, Faculty of Science, Palacký University, 17. listopadu 12, Olomouc, Czech Republic.

Table S1. Crystal data and structure refinement for 1 – 6.....	3
Table S2. Selected bond distances and angles (Å, °) for 1 – 3 .....	5
Table S3. Selected bond distances and angles (Å, °) for 4 – 6. ....	6
Table S4. Selected hydrogen bond interactions in 1 – 6 (Å, °).....	7
Table S5. Cg···Cg distances and angles (Å, °) characterizing π–π interactions in 1 – 6. ....	9
Table S6. Parameters of one-component Debye's model for 1 derived according eqn. 6 in the main text.....	10
Table S7. Parameters of one-component Debye's model for 2 derived according eqn. 6 in the main text.....	10
Table S8. Parameters of one-component Debye's model for 4 derived according eqn. 6 in the main text.....	11
Table S9. Parameters of one-component Debye's model for 5 derived according eqn. 6 in the main text.....	11
Table S10. Parameters of one-component Debye's model for 6 derived according eqn. 6 in the main text.....	12
Figure S1. Visualization of the hydrogen bonds in the crystal structure of 1.....	13
Figure S2. Visualization of the hydrogen bonds in the crystal structure of 2.....	14
Figure S3. Visualization of the hydrogen bonds in the crystal structure of 3.....	15

Figure S4. Visualization of the hydrogen bonds in the crystal structure of 4 .....	16
Figure S5. Visualization of the hydrogen bonds in the crystal structure of 5 .....	17
Figure S6. Visualization of the hydrogen bonds hydrogen bonds (top) and $\pi-\pi$ stacking interactions (bottom) in the crystal structure of 6 .....	18
Figure S7. The multiplet energy levels calculated by CASSCF/NEVPT2 (black color) and reconstructed energy levels with the L-S Hamiltonian (eqn. 1) (red color) with $\alpha \cdot \lambda = -223 \text{ cm}^{-1}$ , $\Delta_{\text{ax}} = -1803 \text{ cm}^{-1}$ , $\Delta_{\text{rh}} = -319 \text{ cm}^{-1}$ for 6. ....	19
Figure S8 In-phase $\chi_{\text{real}}$ and out-of-phase $\chi_{\text{imag}}$ molar susceptibilities for 1 at zero static magnetic field (left) and in non-zero static field (right). ....	19
Figure S9 In-phase $\chi_{\text{real}}$ and out-of-phase $\chi_{\text{imag}}$ molar susceptibilities for 2 at zero static magnetic field (left) and in non-zero static field (right). ....	20
Figure S10 In-phase $\chi_{\text{real}}$ and out-of-phase $\chi_{\text{imag}}$ molar susceptibilities for 3 at zero static magnetic field (left) and in non-zero static field (right). ....	21
Figure S11 In-phase $\chi_{\text{real}}$ and out-of-phase $\chi_{\text{imag}}$ molar susceptibilities for 4 at zero static magnetic field (left) and in non-zero static field (right). ....	22
Figure S12 In-phase $\chi_{\text{real}}$ and out-of-phase $\chi_{\text{imag}}$ molar susceptibilities for 5 at zero static magnetic field (left) and in non-zero static field (right). ....	23
Figure S13 In-phase $\chi_{\text{real}}$ and out-of-phase $\chi_{\text{imag}}$ molar susceptibilities for 6 at zero static magnetic field (left) and in non-zero static field (right). ....	24
Figure S14. In-phase $\chi_{\text{real}}$ and out-of-phase $\chi_{\text{imag}}$ molar susceptibilities for 3. The lines serve as guides for the eyes.....	25
Figure S15. AC susceptibility data for 2 .....	26
Figure S16. AC susceptibility data for 4 .....	27
Figure S17. AC susceptibility data for 5 .....	28
Figure S18. Analysis of in-phase $\chi'$ and out-of-phase $\chi''$ molar susceptibilities for 1-6 measured at the applied external field $B_{\text{dc}} = 0.1 \text{ T}$ according to eq. 9 .....	29
Figure S19. Analysis of in-phase $\chi'$ and out-of-phase $\chi''$ molar susceptibilities for 1-6 measured at the applied external field $B_{\text{dc}} = 0.1 \text{ T}$ according to eq. 10 .....	30

**Table S1.** Crystal data and structure refinement for **1 – 6**

Compound	<b>1</b>	<b>2</b>	<b>3</b>	<b>4</b>	<b>5</b>	<b>6</b>
Empirical formula	CoC <sub>36</sub> H <sub>28</sub> N <sub>22</sub> O <sub>4</sub>	CoC <sub>30</sub> H <sub>24</sub> N <sub>18</sub> O <sub>6</sub>	CoC <sub>42</sub> H <sub>28</sub> N <sub>22</sub> O <sub>2</sub>	CoC <sub>26</sub> H <sub>20</sub> N <sub>18</sub> O <sub>4</sub>	CoC <sub>26</sub> H <sub>20</sub> N <sub>14</sub> Se <sub>2</sub>	CoC <sub>30</sub> N <sub>18</sub> H <sub>20</sub> O <sub>2</sub>
Formula weight	891.73	791.60	931.79	707.53	745.41	723.57
Temperature [K]	173(2)	173(2)	173(2)	173	173(2)	173(2)
Wavelength [Å]	0.71073	0.71073	0.71073	0.71073	0.71073	0.71073
Crystal system	Triclinic	Monoclinic	Triclinic	Monoclinic	Monoclinic	Triclinic
Space group	<i>P</i> -1	<i>P</i> 2 <sub>1</sub> /c	<i>P</i> -1	<i>P</i> 2 <sub>1</sub> /c	<i>P</i> 2 <sub>1</sub> /c	<i>P</i> -1
Unit cell dimensions [Å, °]	<i>a</i> = 8.0992(8)		<i>a</i> = 7.1594(2)			<i>a</i> = 9.0417(4)
	<i>b</i> = 11.4165(10)	<i>a</i> = 7.6946(3)	<i>b</i> = 12.3043(4)	<i>a</i> = 8.6207(6)	<i>a</i> = 8.5646(4)	<i>b</i> = 9.8054(4)
	<i>c</i> = 11.7630(11)	<i>b</i> = 13.5526(6)	<i>c</i> = 12.9843(4)	<i>b</i> = 16.5927(11)	<i>b</i> = 10.1344(3)	<i>c</i> = 9.8315(4)
	$\alpha$ = 103.655(8)	<i>c</i> = 16.7231(8)	$\alpha$ = 71.278(3)	<i>c</i> = 10.1837(6)	<i>c</i> = 19.0783(8)	$\alpha$ = 86.688(3)
	$\beta$ = 103.501(8)	$\beta$ = 101.741(4)	$\beta$ = 75.397(2)	$\beta$ = 94.343(6)	$\beta$ = 119.986(5)	$\beta$ = 63.486(4)
	$\gamma$ = 97.011(8)		$\gamma$ = 83.503(2)			$\gamma$ = 82.592(4)
Volume [Å <sup>3</sup> ]	1009.48(17)	1707.43(13)	1047.64(6)	1452.50(16)	1434.29(12)	773.45(6)
Z; calculated density [g.cm <sup>-3</sup> ]	1; 1.467	2; 1.540	1; 1.477	2; 1.618	2; 1.726	1; 1.553
Absorption coefficient [mm <sup>-1</sup> ]	0.496	0.576	0.478	0.662	3.181	0.619
<i>F</i> (000)	457	810	477	722	738	369
Crystal shape, color	prism, yellow	needle, yellow	prism, yellow	prism, yellow	prism, yellow	needle, orange
Crystal size [mm <sup>3</sup> ]	0.46 x 0.34 x 0.22	0.56 x 0.15 x 0.10	0.61 x 0.34 x 0.10	0.29 x 0.15 x 0.15	0.42 x 0.25 x 0.15	0.54 x 0.22 x 0.16
$\theta$ range for data collection [°]	2.97 – 26.50	3.01 – 26.50	3.04 – 26.50	3.17 – 26.50	3.12 – 26.50	3.10 – 26.50
Index ranges	-10 ≤ <i>h</i> ≤ 10	-9 ≤ <i>h</i> ≤ 9	-8 ≤ <i>h</i> ≤ 8	-10 ≤ <i>h</i> ≤ 10	-10 ≤ <i>h</i> ≤ 10	-11 ≤ <i>h</i> ≤ 11
	-14 ≤ <i>k</i> ≤ 14	-15 ≤ <i>k</i> ≤ 17	-15 ≤ <i>k</i> ≤ 15	-20 ≤ <i>k</i> ≤ 20	-12 ≤ <i>k</i> ≤ 12	-12 ≤ <i>k</i> ≤ 12
	-14 ≤ <i>l</i> ≤ 14	-20 ≤ <i>l</i> ≤ 19	-16 ≤ <i>l</i> ≤ 16	-12 ≤ <i>l</i> ≤ 12	-23 ≤ <i>l</i> ≤ 23	-12 ≤ <i>l</i> ≤ 12
Reflections collected/independent	10541 / 4180	10955 / 3536	17611 / 4330	5088 / 5088	11569 / 2930	12862 / 3212
<i>T</i> <sub>min</sub> , <i>T</i> <sub>max</sub>	[ <i>R</i> <sub>int</sub> = 0.0249]	[ <i>R</i> <sub>int</sub> = 0.0217]	[ <i>R</i> <sub>int</sub> = 0.0231]	[ <i>R</i> <sub>int</sub> = 0.0317]	[ <i>R</i> <sub>int</sub> = 0.0235]	[ <i>R</i> <sub>int</sub> = 0.0269]
	0.853, 0.907	0.814, 0.944	0.830, 0.953	0.936, 1.000	0.408, 0.657	0.813, 0.914
Data/restraints/parameters	4180/0/311	3536/0/266	4330/0/328	5088/0/232	2930/0/204	3212/0/240
Goodness-of-fit on <i>F</i> <sup>2</sup>	1.065	1.056	1.048	1.046	1.042	1.085

Final $R$ indices	$R_1 = 0.0306$	$R_1 = 0.0356$	$R_1 = 0.0312$	$R_1 = 0.0365$	$R_1 = 0.0355$	$R_1 = 0.0340$
[ $I > 2\sigma(I)$ ]	$wR_2 = 0.0662$	$wR_2 = 0.0896$	$wR_2 = 0.0732$	$wR_2 = 0.0851$	$wR_2 = 0.0892$	$wR_2 = 0.0794$
$R$ indices (all data)	$R_1 = 0.0395$	$R_1 = 0.0470$	$R_1 = 0.0372$	$R_1 = 0.0675$	$R_1 = 0.0420$	$R_1 = 0.0419$
	$wR_2 = 0.0700$	$wR_2 = 0.0958$	$wR_2 = 0.0764$	$wR_2 = 0.0922$	$wR_2 = 0.0934$	$wR_2 = 0.0831$
Largest diff. peak and hole [e. $\text{\AA}^3$ ]	0.237; -0.309	0.236; -0.467	0.610; -0.286	0.460; -0.332	0.962; -0.611	0.359; -0.381

**Table S2.** Selected bond distances and angles ( $\text{\AA}$ ,  $^\circ$ ) for **1 – 3**.

<i>Bond distances</i>	<b>1</b>	<b>2</b>	<b>3</b>	<i>Bond angles</i>	<b>1</b>	<b>2</b>	<b>3</b>
Co1–N10	2.081(1)	2.112(2)	2.058(1)	N10–Co1–N50 <sup>i</sup>	76.72(5)	77.07(6)	103.15(5)
Co1–N50	2.166(1)	2.146(2)	2.151(1)	N10–Co1–N50	103.27(5)	102.93(6)	76.86(5)
Co1–O1	2.102	2.118(2)	2.109(1)	N10–Co1–O1	90.68(5)	89.70(7)	89.59(5)
C1–N1	1.325(2)			N50–Co1–O1	88.86(5)	90.13(6)	87.21(5)
C2–N2	1.153(2)	1.145(3)	1.149(2)	N50–Co1–O1 <sup>i</sup>	91.15(5)	89.87(6)	92.79(5)
C3–N3	1.150(2)	1.143(3)		N10–Co1–O1 <sup>i</sup>	89.32(5)	90.30(7)	90.41(5)
C4–N1	1.332(2)			C1–N1–C4	127.13(14)		
C5–N5	1.150(2)		1.138(2)	N1–C1–C3	127.33(15)		
C6–N6	1.150(2)			N1–C1–C2	116.69(15)		
C1–C3	1.433(2)	1.418(3)	1.378(3)	C3–C1–C2	115.93(14)	123.2(2)	115.35(16)
C1–C2	1.436(2)	1.407(3)	1.477(2)	N3–C3–C1	177.05(18)	178.8(3)	
C4–C6	1.433(2)			N2–C2–C1	178.65(19)	179.6(3)	177.4(2)
C4–C5	1.438(2)			N1–C4–C6	116.13(14)		
C1–N4	-	1.363(3)		N1–C4–C5	127.39(15)		
N4–O2		1.237(2)		C6–C4–C5	116.47(14)		
N4–O3		1.260(2)		N6–C6–C4	179.33(18)		
C1–C6		1.397(2)		N5–C5–C4	178.37(17)		
C3–C4		1.441(3)		N4–C1–C2		118.07(19)	
C3–C5		1.419(2)		N4–C1–C3		118.65(19)	
C6–C7		1.429(3)		O2–N4–O3		122.61(18)	
C6–C8		1.427(2)		O2–N4–C1		119.60(18)	
C4–N4		1.147(3)		O3–N4–C1		117.77(17)	
C7–N7		1.152(3)		C1–C6–C8			124.34(16)
C8–N8		1.148(2)		C1–C6–C7			119.64(15)
				C8–C6–C7			115.97(15)
				C3–C1–C6			129.67(17)
				C6–C1–C2			114.98(16)
				N8–C8–C6			176.53(19)
				N5–C5–C3			175.7(2)
				C1–C3–C5			123.39(17)
				C1–C3–C4			120.72(16)
				C5–C3–C4			115.89(17)
				N7–C7–C6			178.8(2)
				N4–C4–C3			176.7(2)

[Symmetry codes: (i)  $1 - x, 1 - y, 1 - z$  (**1**); (i)  $1 - x, 1 - y, -z$  (**2, 3**)]

**Table S3.** Selected bond distances and angles ( $\text{\AA}$ ,  $^\circ$ ) for **4 – 6**.

<i>Bond distances</i>	<b>4</b>	<b>5</b>	<b>6</b>	<i>Bond angles</i>	<b>4</b>	<b>5</b>	<b>6</b>
Co1–N10	2.086(2)	2.086(3)	2.104(2)	N10–Co1–N50 <sup>i</sup>	103.03(8)	76.09(10)	77.23(6)
Co1–N50	2.144(2)	2.165(2)	2.142(2)	N10–Co1–N50	76.97(8)	103.91(10)	102.77(6)
Co1–N1	2.121(2)	2.121(3)		N10–Co1–N1	89.95(8)	91.98(10)	
Co1–O1			2.092 (1)	N10–Co1–N1 <sup>i</sup>	90.05(8)	88.02(10)	
N1–O1			1.289(2)	N50–Co1–N1 <sup>i</sup>	90.04(8)	89.59(9)	
N3–O2	1.230(3)			N50–Co1–N1	89.96(8)	90.42(9)	
N3–O1	1.233(3)			N10–Co1–O1			84.66(6)
C1–N1	1.142(3)	1.155(4)	1.333(3)	N50–Co1–O1			91.09(6)
N2–N3	1.354(3)			N50–Co1–O1 <sup>i</sup>			88.91(6)
C1–N2	1.325(3)			N10–Co1–O1 <sup>i</sup>			95.34(6)
C1–Se1		1.805(3)		O2–N3–O1	123.2(2)		
C3–N3			1.145(3)	O2–N3–N2	121.0(2)		
C2–N2			1.137(3)	O1–N3–N2	115.7(2)		
C1–C3			1.427(3)	C1–N2–N3	112.4(2)		115.35(16)
C1–C2			1.430(3)	N1–C1–N2	173.1(3)		
				N1–C1–Se1		178.5(3)	177.4(2)
				O1–N1–C1			113.48(17)
				N1–C1–C3			117.97(19)
				N1–C1–C2			123.2(2)
				C3–C1–C2			118.76(19)
				N2–C2–C1			179.2(3)
				N3–C3–C1			176.4(2)

[Symmetry codes: (i)  $1 - x, 1 - y, -z$  (**4**); (i)  $-x, -y, -z$  (**5**); (i)  $1 - x, -y, 1 - z$  (**6**)

**Table S4.** Selected hydrogen bond interactions in **1 – 6** (Å, °).

Compound	Donor–H···Acceptor	D–H	H···A	D···A	< D–H···A
<b>1</b>	O1–H1O1···N2 <sup>ii</sup>	0.82(2)	2.08(2)	2.863(2)	160(2)
	O1–H2O1···O2	0.82(2)	1.91(2)	2.726(2)	172(2)
	N40–H1N···O2 <sup>iii</sup>	0.91(2)	2.14(2)	3.045(2)	172 (2)
	O2–H1O2···N6 <sup>iv</sup>	0.83(2)	2.07(2)	2.889(2)	169(2)
	O2–H2O2···N1	0.81(2)	2.13(2)	2.931(2)	174(2)
	N40–H2N···N60	0.91(2)	2.09(2)	2.838(2)	139(2)
<b>2</b>	N40–H2N···N3 <sup>i</sup>	0.94(3)	2.36(3)	3.200(4)	149(3)
	O1–H1O···N2 <sup>ii</sup>	0.81(3)	2.07(3)	2.873(3)	174(3)
	O1–H2O···O3	0.85(3)	1.88(3)	2.719(2)	168(3)
	N40–H1N···O2 <sup>ii</sup>	0.90(3)	2.49(3)	3.204(3)	136(2)
	N40–H1N···N2 <sup>iii</sup>	0.90(3)	2.54(3)	3.096(3)	120(2)
	N40–H1N···N60	0.90(3)	2.42(3)	2.861(3)	110(2)
<b>3</b>	O1–H1O···N8	0.78(2)	2.07(2)	2.846(2)	174(2)
	N40–H2N···N5	0.90(2)	2.39(2)	3.155(3)	142(2)
	C54–H54···N7 <sup>ii</sup>	0.95	2.55	3.256(2)	131
	N40–H1N···N60	0.85(3)	2.16(2)	2.863(2)	140(2)
<b>4</b>	N40–H1N···O2 <sup>ii</sup>	0.85(3)	2.51(3)	2.810(3)	102(2)
	N40–H2N···N2 <sup>iii</sup>	0.87(3)	2.26(3)	3.033(3)	147(2)

	N40—H1N···N60	0.85(3)	2.23(3)	2.871(4)	132(3)
<b>5</b>	N40—H1N···Se <sup>ii</sup>	0.93(5)	2.76(5)	3.524(3)	139(3)
	N40—H1N···N60	0.94(5)	2.10(6)	2.851(5)	135(4)
<b>6</b>	N40—H1N···N3 <sup>ii</sup>	0.89(3)	2.39(2)	3.138(3)	142 (2)
	N40—H2N···N60	0.87(3)	2.24(3)	2.891(3)	131(3)

[Symmetry codes: (ii)  $-x, 1-y, 1-z$ ; (iii)  $1+x, y, z$ ; (iv)  $1-x, 2-y, 1-z$  (**1**); (ii)  $1-x, -0.5+y, 0.5-z$ ; (iii)  $x, -1+y, z$  (**2**); (ii)  $1-x, -y, 1-z$  (**3**); (ii)  $1-x, 1-y, 1-z$ ; (iii)  $1-x, 0.5+y, 0.5-z$  (**4**); (ii)  $1-x, -0.5+y, 0.5-z$  (**5**); (ii)  $2-x, -y, -z$  (**6**)]

**Table S5.** Cg···Cg distances and angles ( $\text{\AA}$ ,  $^\circ$ ) characterizing  $\pi$ – $\pi$  interactions in **1** – **6**.

Compound	Cg(I)···Cg(J)	Cg···Cg	$\alpha^{\text{a}}$	$\beta$	$\gamma$
<b>1</b>	Cg1···Cg1 <sup>v</sup>	3.730(1)	0	21.9	21.9
<b>2</b>	Cg2···Cg1 <sup>iv</sup>	3.695(1)	0.80(10)	23.6	23.1
<b>3</b>	Cg1···Cg1 <sup>iii</sup>	3.895(1)	0.02(9)	25.8	25.8
	Cg1···Cg1 <sup>iv</sup>	3.845(1)	0.02(9)	27.6	27.6
<b>4</b>	Cg1···Cg2 <sup>ii</sup>	3.745(2)	2.20(12)	23.9	26.1
<b>5</b>	Cg1···Cg2 <sup>iii</sup>	3.651(2)	9.22(16)	30.9	21.7
<b>6</b>	Cg1···Cg1 <sup>iii</sup>	3.518(1)	0.02(9)	16.9	16.9
	Cg2···Cg1 <sup>iv</sup>	3.642(1)	16.90(9)	30.1	15.0

[Symmetry codes: (v)  $2 - x, 1 - y, -z$  (**1**); (iv)  $-x, 1 - y, -z$  (**2**); (iii)  $1 - x, 2 - y, -z$ ; (iv)  $2 - x, 2 - y, -z$  (**3**); (ii)  $1 - x, 1 - y, 1 - z$  (**4**); (iii)  $x, -1 + y, z$  (**5**); (iii)  $1 - x, -1 - y, -z$ ; (iv)  $x, 1 + y, z$  (**6**)]

Cg1 represents centroid of the uncoordinated pyridyl ring containing N60 atom

Cg2 represents centroid of the coordinated pyridyl ring containing N50 atom

<sup>a</sup> $\alpha$  is the dihedral angle between planes I and J.  $\beta$  is the angle between Cg(I)···Cg(J) vector

and normal to plane I.  $\gamma$  is the angle between Cg(I)···Cg(J) vector and normal to plane J

**Table S6.** Parameters of one-component Debye's model for **1** derived according eqn. 6 in the main text.

T/K	$\chi_S/(m^3 \text{ mol}^{-1})$	$\chi_T/(m^3 \text{ mol}^{-1})$	$\alpha$	$\tau/(s)$
1.9	4.77E-07	9.71E-06	1.50E-01	2.46E-02
2.2	4.56E-07	8.29E-06	1.25E-01	1.80E-02
2.5	4.20E-07	7.35E-06	1.38E-01	1.34E-02
2.8	4.11E-07	6.52E-06	1.05E-01	9.58E-03
3.1	4.11E-07	5.87E-06	7.55E-02	6.90E-03
3.4	3.62E-07	5.36E-06	8.48E-02	4.76E-03
3.7	3.25E-07	4.93E-06	5.87E-02	3.32E-03
4.0	3.81E-07	4.56E-06	4.78E-02	2.38E-03
4.3	3.36E-07	4.25E-06	3.94E-02	1.59E-03
4.6	3.66E-07	4.00E-06	2.95E-02	1.17E-03
4.9	3.46E-07	3.77E-06	1.34E-02	8.06E-04
5.2	3.04E-07	3.57E-06	2.46E-02	5.30E-04
5.5	3.51E-07	3.38E-06	1.21E-02	3.43E-04
5.8	1.42E-07	3.22E-06	5.32E-02	1.96E-04

**Table S7.** Parameters of one-component Debye's model for **2** derived according eqn. 6 in the main text.

T/K	$\chi_S/(m^3 \text{ mol}^{-1})$	$\chi_T/(m^3 \text{ mol}^{-1})$	$\alpha$	$\tau/(s)$
1.9	4.42E-07	8.95E-06	1.05E-01	3.72E-03
2.2	4.16E-07	7.77E-06	1.07E-01	2.70E-03
2.5	3.62E-07	6.90E-06	9.14E-02	2.08E-03
2.8	3.68E-07	6.18E-06	1.12E-01	1.62E-03
3.1	3.82E-07	5.59E-06	9.13E-02	1.30E-03
3.4	3.79E-07	5.10E-06	7.58E-02	1.01E-03
3.7	3.46E-07	4.72E-06	7.27E-02	8.18E-04
4.0	3.40E-07	4.39E-06	8.23E-02	6.32E-04
4.3	3.85E-07	4.09E-06	3.81E-02	5.15E-04

**Table S8.** Parameters of one-component Debye's model for **4** derived according eqn. 6 in the main text.

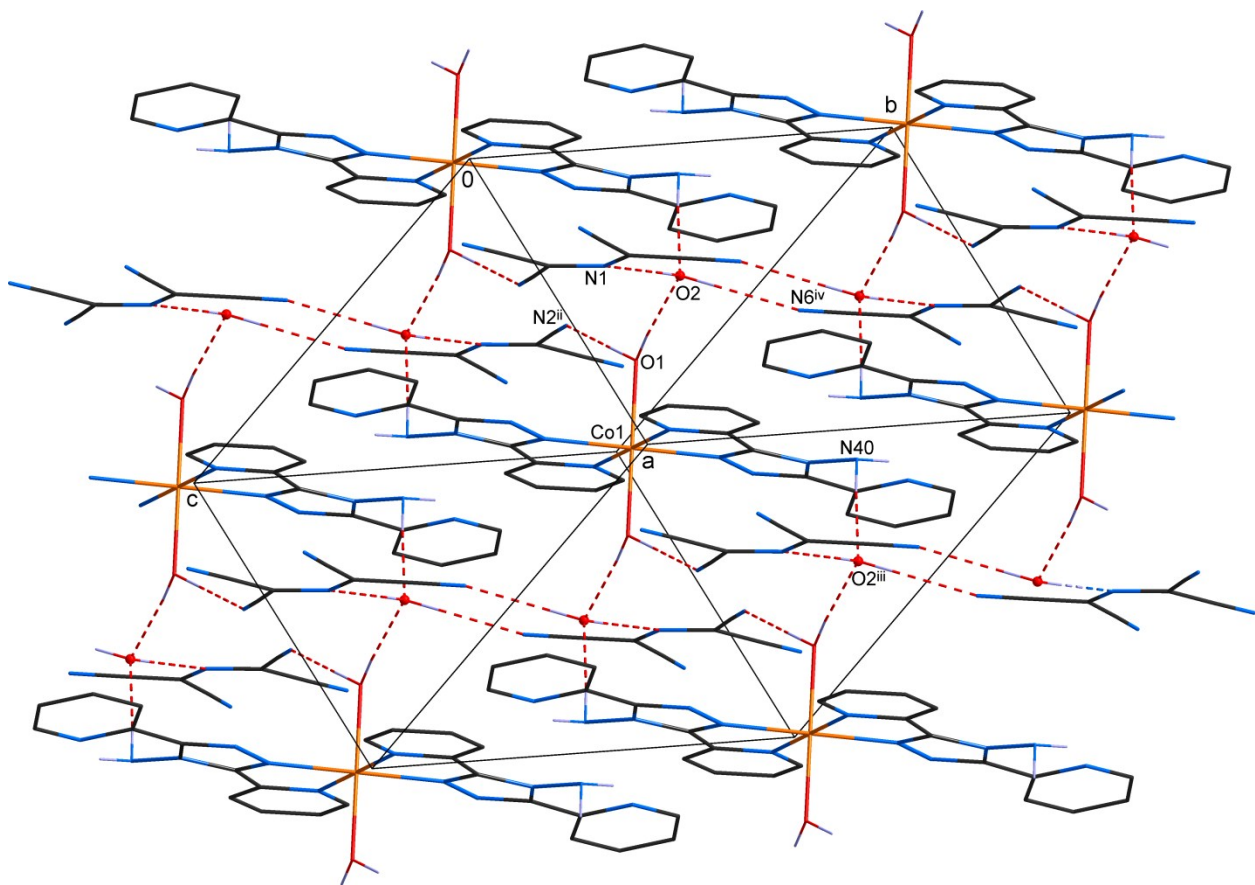
T/K	$\chi_S/(m^3 mol^{-1})$	$\chi_T/(m^3 mol^{-1})$	$\alpha$	$\tau/(s)$
1.9	5.83E-07	1.02E-05	1.45E-01	1.19E-03
2.2	6.54E-07	9.02E-06	1.25E-01	9.70E-04
2.5	6.81E-07	8.01E-06	1.12E-01	8.07E-04
2.8	6.48E-07	7.13E-06	1.01E-01	6.59E-04
3.1	7.19E-07	6.48E-06	9.01E-02	5.79E-04
3.4	8.73E-07	5.89E-06	3.01E-02	5.27E-04
3.7	8.02E-07	5.46E-06	5.98E-02	4.36E-04
4.0	7.17E-07	5.07E-06	6.42E-02	3.87E-04
4.3	8.52E-07	4.73E-06	2.95E-02	3.56E-04
4.6	8.99E-07	4.44E-06	4.65E-02	3.08E-04
4.9	6.89E-07	4.18E-06	5.25E-02	2.54E-04
5.2	7.29E-07	3.95E-06	4.39E-02	2.21E-04

**Table S9.** Parameters of one-component Debye's model for **5** derived according eqn. 6 in the main text.

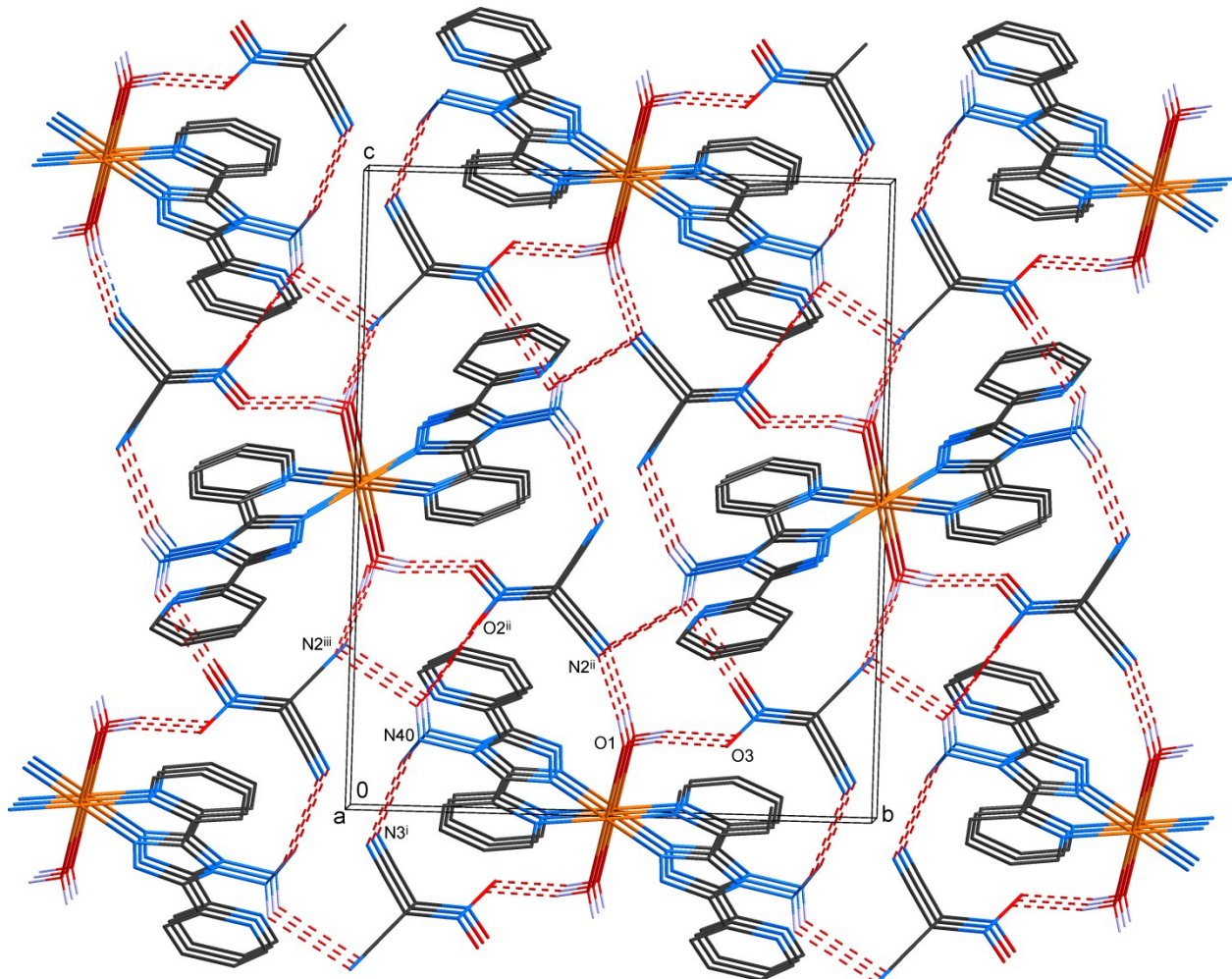
T/K	$\chi_S/(m^3 mol^{-1})$	$\chi_T/(m^3 mol^{-1})$	$\alpha$	$\tau/(s)$
1.9	4.71E-07	1.06E-05	1.77E-01	2.10E-03
2.2	4.15E-07	9.30E-06	1.85E-01	1.50E-03
2.5	4.12E-07	8.19E-06	1.72E-01	1.09E-03
2.8	4.28E-07	7.32E-06	1.56E-01	8.52E-04
3.1	4.28E-07	6.64E-06	1.45E-01	6.84E-04
3.4	4.06E-07	6.10E-06	1.47E-01	5.66E-04
3.7	4.00E-07	5.62E-06	1.48E-01	4.63E-04
4.0	5.43E-07	5.22E-06	1.12E-01	4.13E-04
4.3	5.27E-07	4.87E-06	1.20E-01	3.37E-04
4.6	6.03E-07	4.56E-06	9.60E-02	3.02E-04
4.9	6.50E-07	4.32E-06	8.31E-02	2.60E-04
5.2	5.34E-07	4.07E-06	9.62E-02	2.06E-04
5.5	4.45E-07	3.86E-06	7.71E-02	1.66E-04

**Table S10.** Parameters of one-component Debye's model for **6** derived according eqn. 6 in the main text.

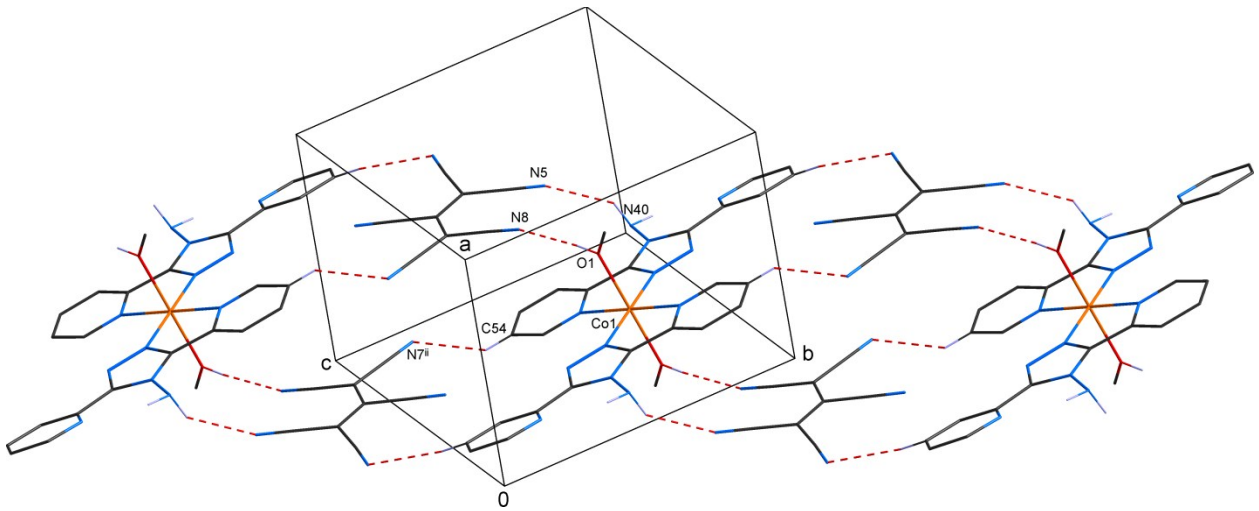
<i>T/K</i>	$\chi_S/(m^3 \text{ mol}^{-1})$	$\chi_T/(m^3 \text{ mol}^{-1})$	$\alpha$	$\tau/(s)$
1.9	8.49E-07	1.07E-05	2.65E-01	4.22E-03
2.2	8.94E-07	9.28E-06	2.32E-01	3.19E-03
2.5	7.95E-07	8.12E-06	2.09E-01	2.34E-03
2.8	6.58E-07	7.28E-06	2.35E-01	1.73E-03
3.1	6.58E-07	6.54E-06	2.10E-01	1.32E-03
3.4	5.79E-07	5.97E-06	1.96E-01	1.02E-03
3.7	6.97E-07	5.49E-06	1.69E-01	8.63E-04
4.0	6.49E-07	5.09E-06	1.58E-01	7.01E-04
4.3	6.84E-07	4.76E-06	1.40E-01	5.92E-04
4.6	6.30E-07	4.45E-06	1.58E-01	4.66E-04
4.9	6.37E-07	4.19E-06	1.40E-01	3.89E-04
5.2	8.76E-07	3.95E-06	6.03E-02	3.90E-04
5.5	8.60E-07	3.75E-06	8.03E-02	2.96E-04
5.8	5.62E-07	3.56E-06	6.08E-02	2.14E-04
6.1	7.01E-07	3.39E-06	8.88E-02	1.77E-04



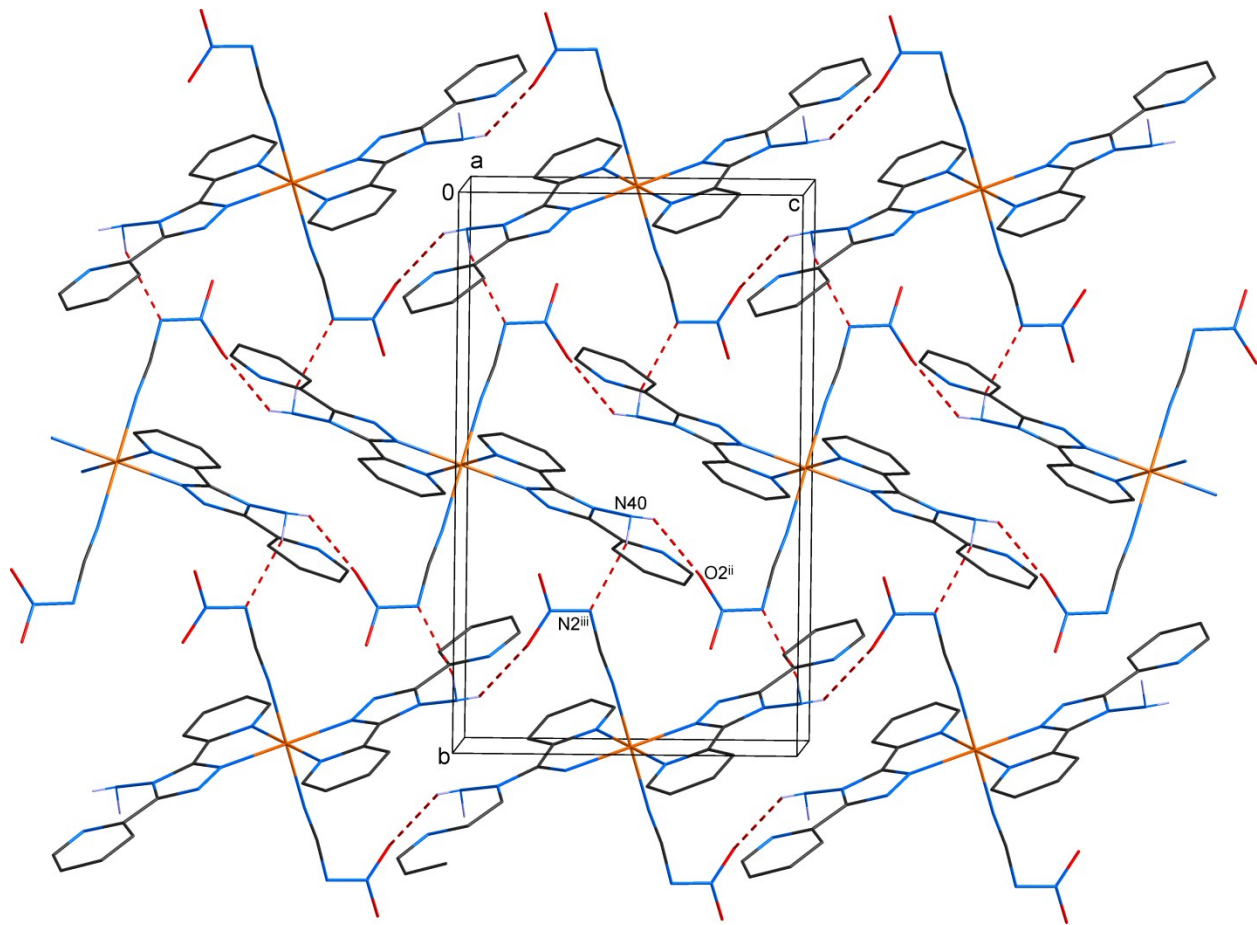
**Figure S1.** Visualization of the selected hydrogen bonds in the crystal structure of **1**.



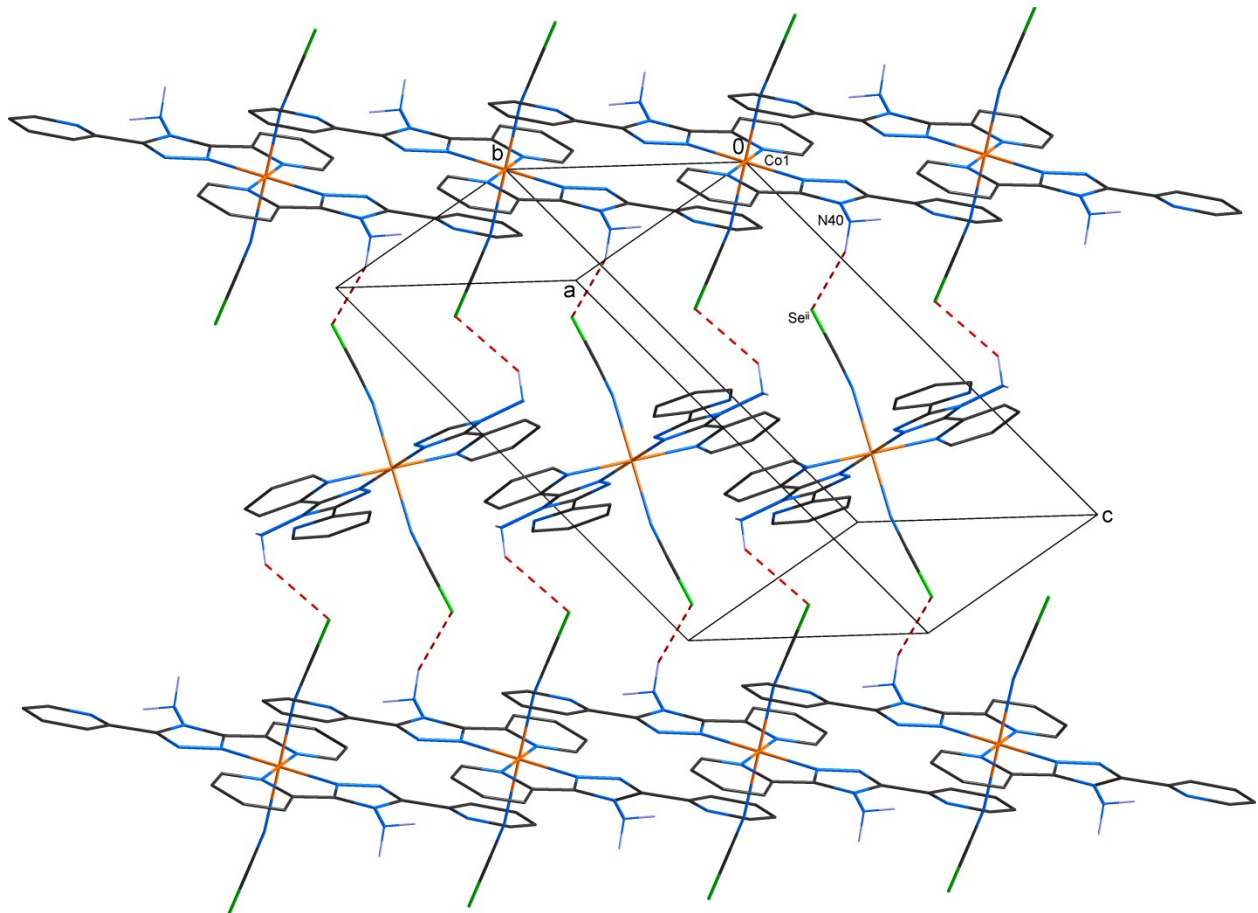
**Figure S2.** Visualization of the selected hydrogen bonds in the crystal structure of **2**.



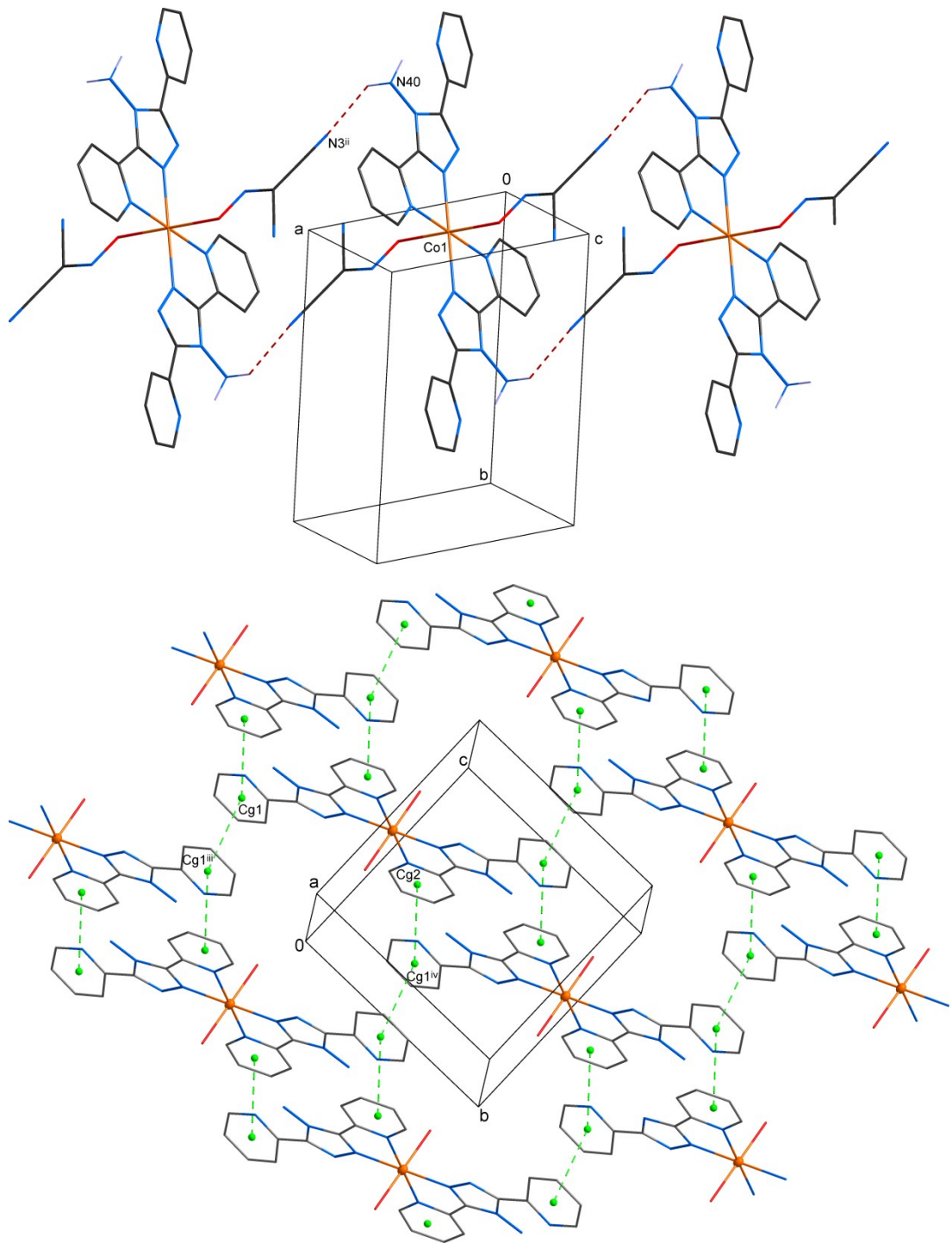
**Figure S3.** Visualization of the selected hydrogen bonds in the crystal structure of **3**.



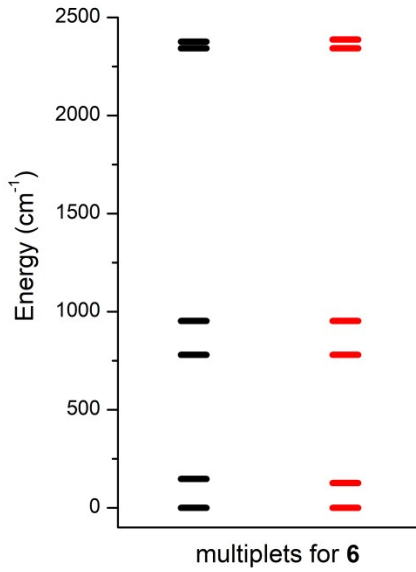
**Figure S4.** Visualization of the selected hydrogen bonds in the crystal structure of **4**.



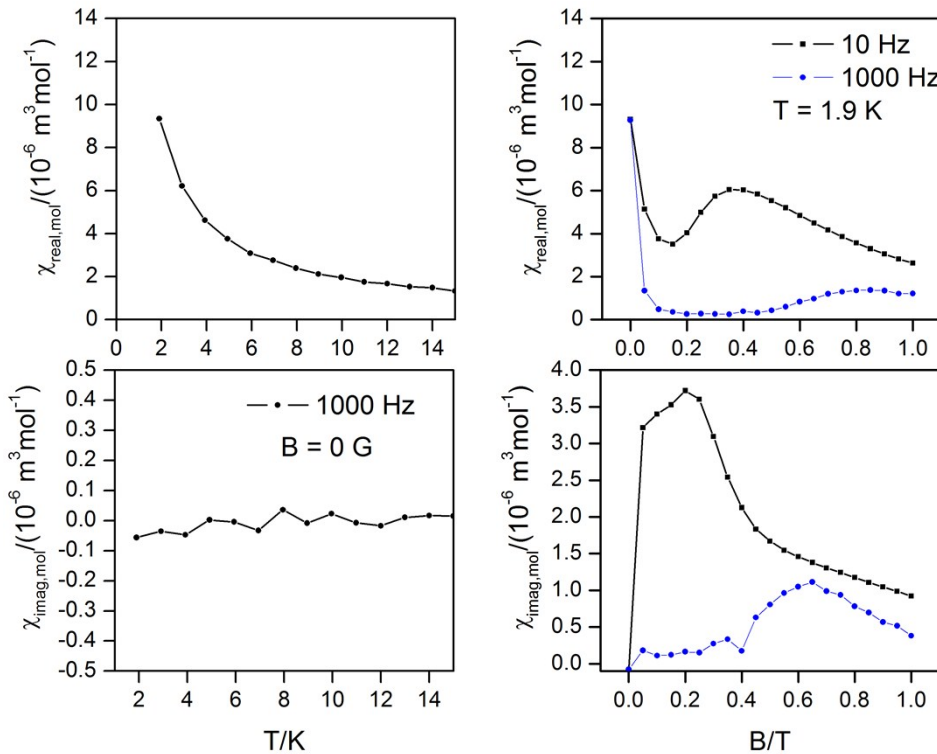
**Figure S5.** Visualization of the selected hydrogen bonds in the crystal structure of **5**.



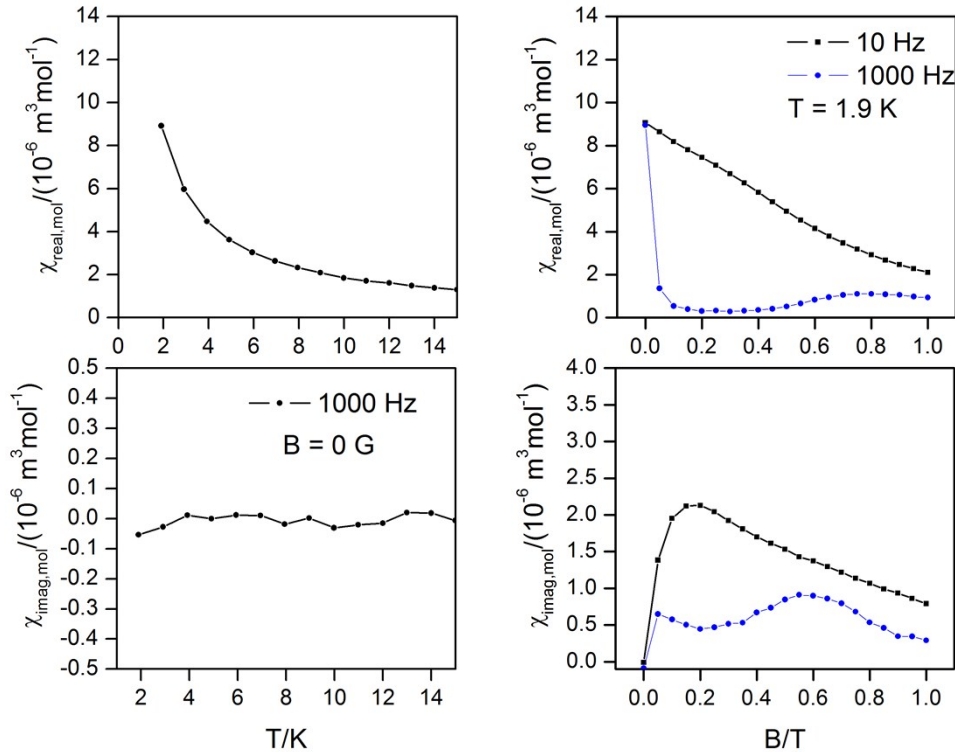
**Figure S6.** Visualization of the selected hydrogen bonds (top) and  $\pi-\pi$  stacking interactions (bottom) in the crystal structure of **6**.



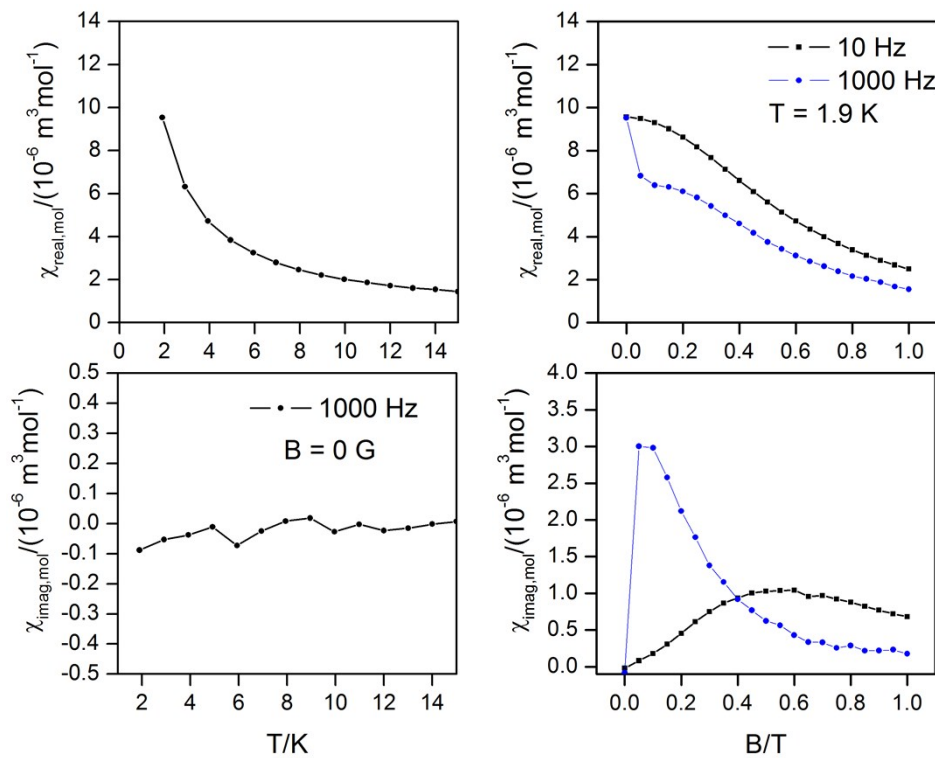
**Figure S7.** The multiplet energy levels calculated by CASSCF/NEVPT2 (black color) and reconstructed energy levels with the L-S Hamiltonian (eqn. 1) (red color) with  $\alpha \cdot \lambda = -223\text{ cm}^{-1}$ ,  $\Delta_{\text{ax}} = -1803\text{ cm}^{-1}$ ,  $\Delta_{\text{rh}} = -319\text{ cm}^{-1}$  for **6**.



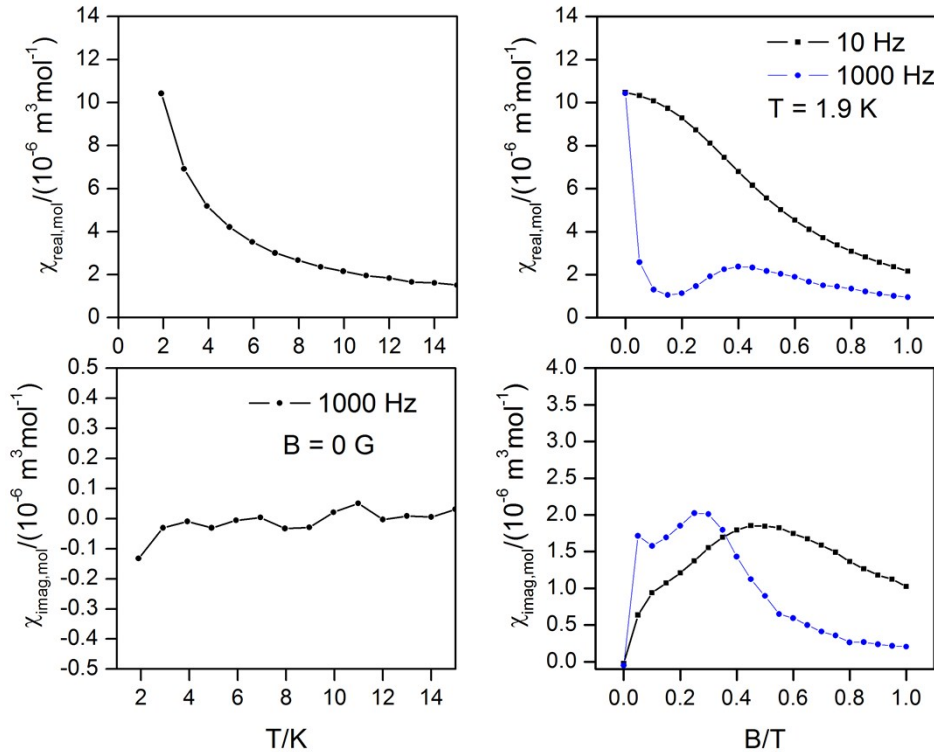
**Figure S8** In-phase  $\chi_{\text{real}}$  and out-of-phase  $\chi_{\text{imag}}$  molar susceptibilities for **1** at zero static magnetic field (*left*) and in non-zero static field (*right*). Lines serve as guides for the eyes.



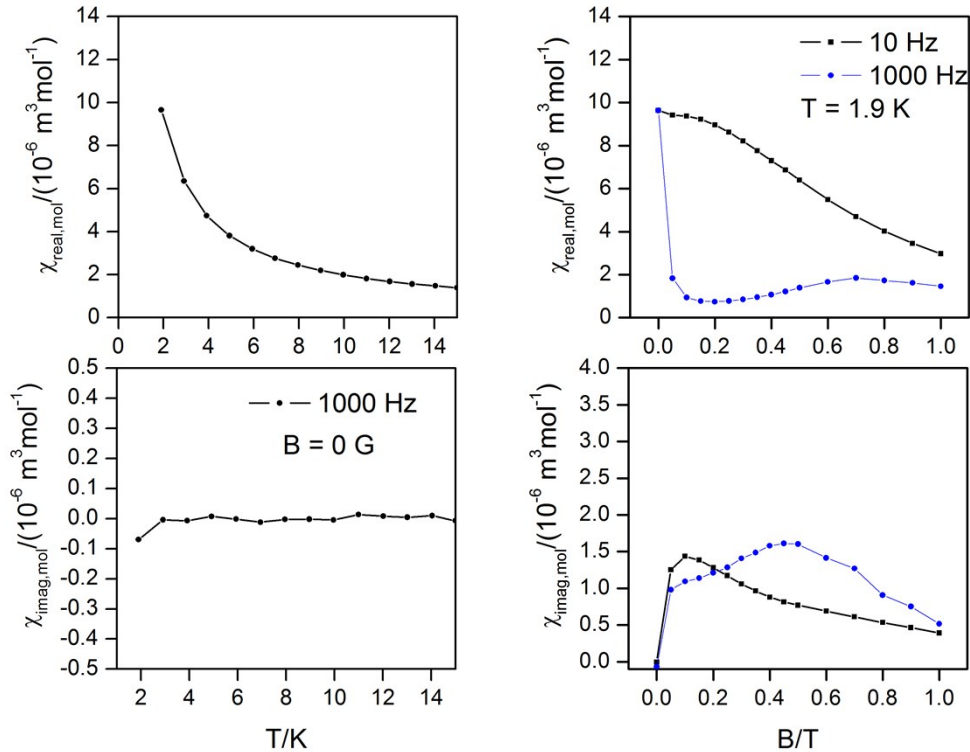
**Figure S9** In-phase  $\chi_{\text{real}}$  and out-of-phase  $\chi_{\text{imag}}$  molar susceptibilities for **2** at zero static magnetic field (*left*) and in non-zero static field (*right*). Lines serve as guides for the eyes.



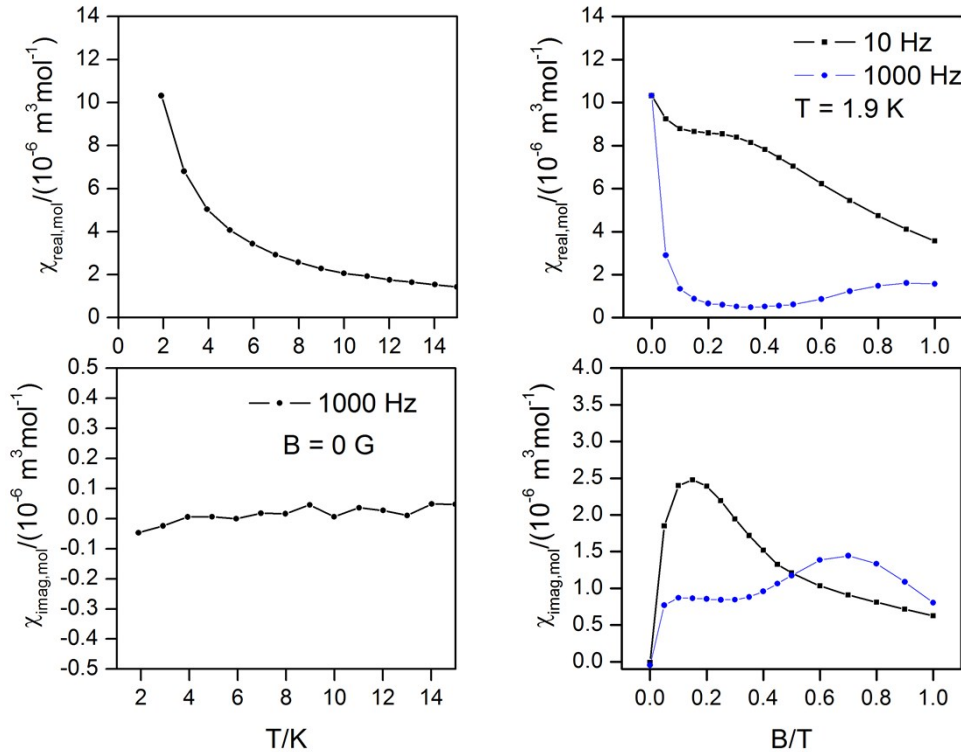
**Figure S10** In-phase  $\chi_{\text{real}}$  and out-of-phase  $\chi_{\text{imag}}$  molar susceptibilities for **3** at zero static magnetic field (*left*) and in non-zero static field (*right*). Lines serve as guides for the eyes.



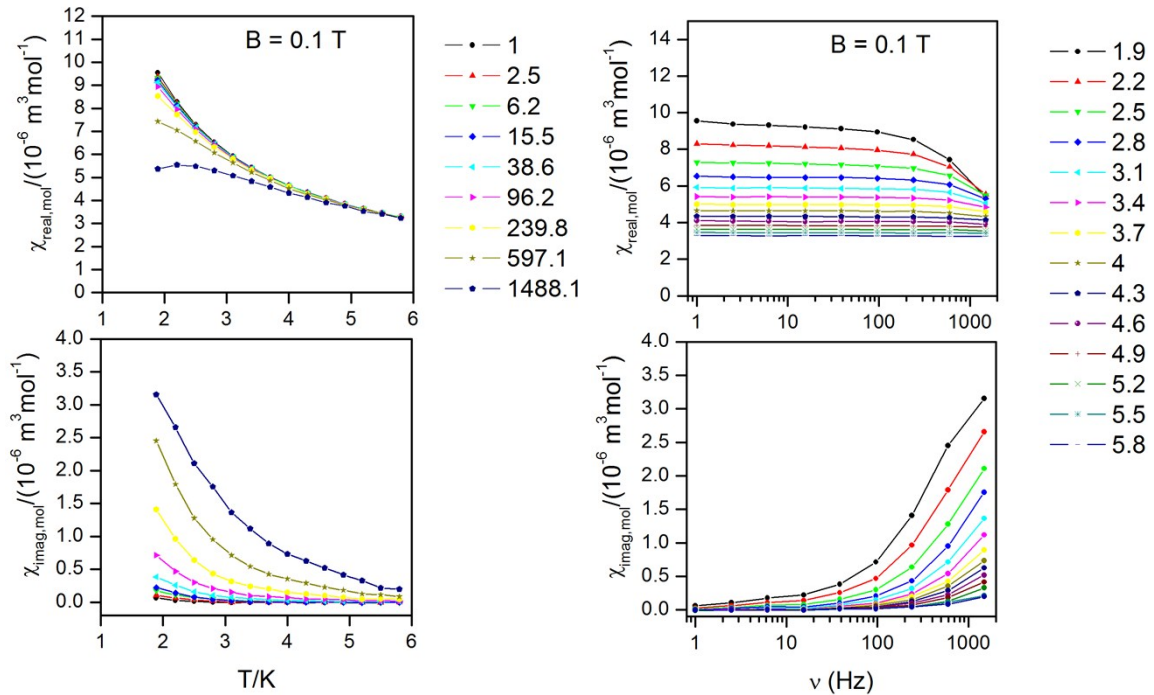
**Figure S11** In-phase  $\chi_{\text{real}}$  and out-of-phase  $\chi_{\text{imag}}$  molar susceptibilities for **4** at zero static magnetic field (*left*) and in non-zero static field (*right*). Lines serve as guides for the eyes.



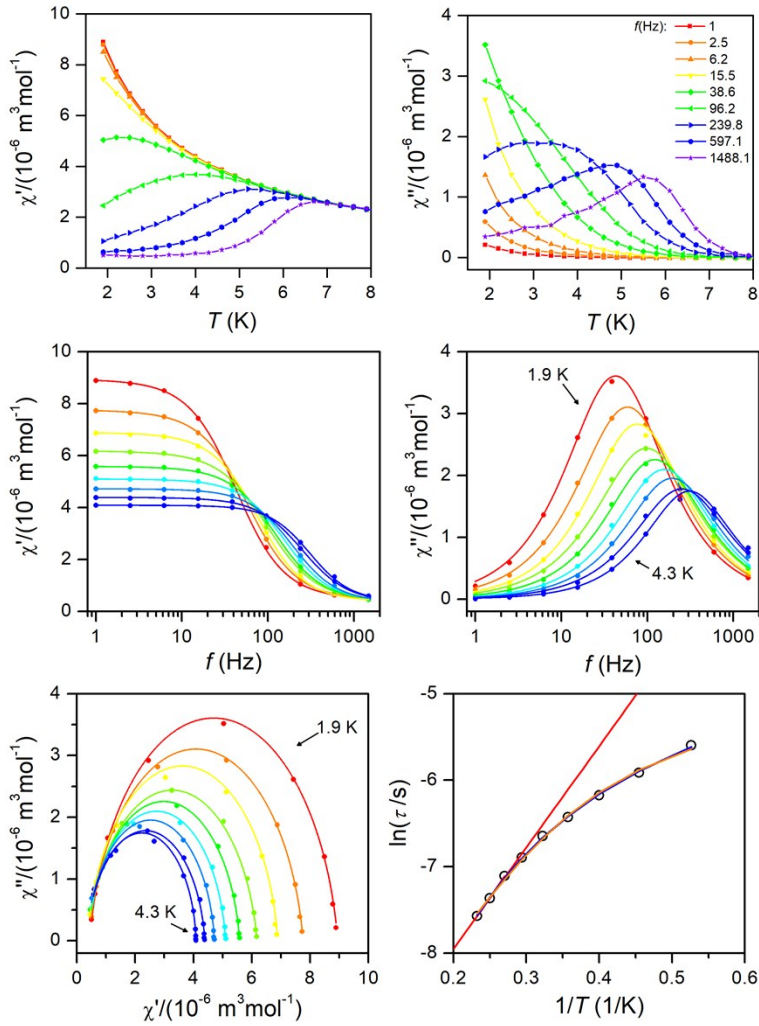
**Figure S12** In-phase  $\chi_{\text{real}}$  and out-of-phase  $\chi_{\text{imag}}$  molar susceptibilities for **5** at zero static magnetic field (*left*) and in non-zero static field (*right*). Lines serve as guides for the eyes.



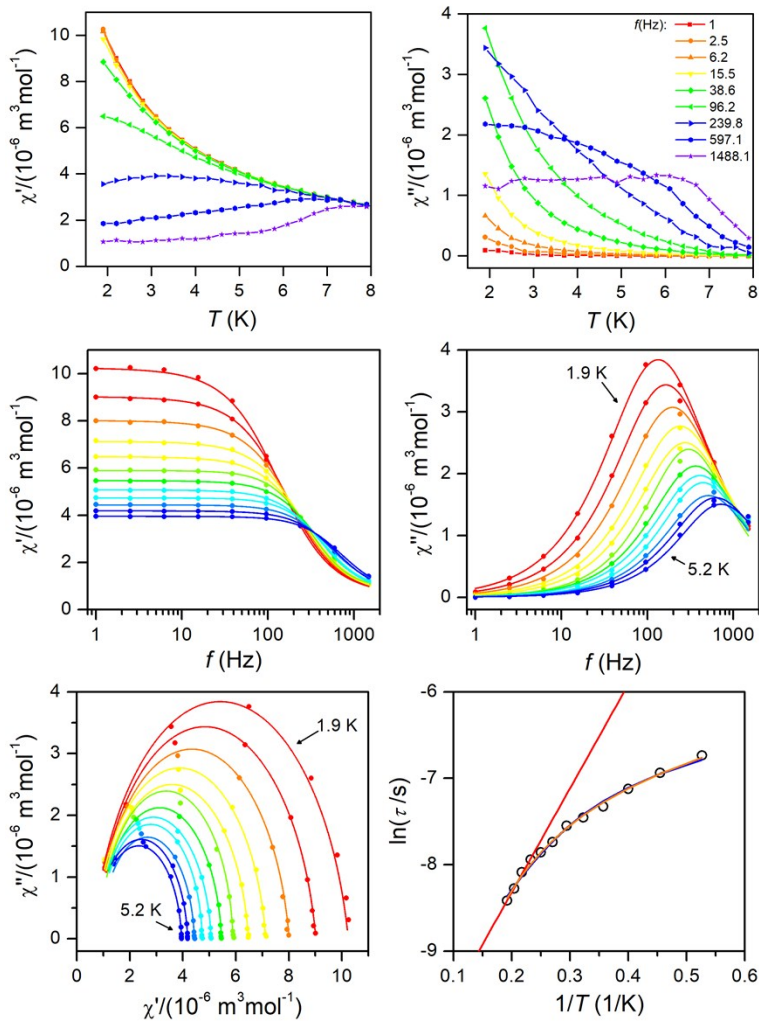
**Figure S13** In-phase  $\chi_{\text{real}}$  and out-of-phase  $\chi_{\text{imag}}$  molar susceptibilities for 6 at zero static magnetic field (*left*) and in non-zero static field (*right*). Lines serve as guides for the eyes.



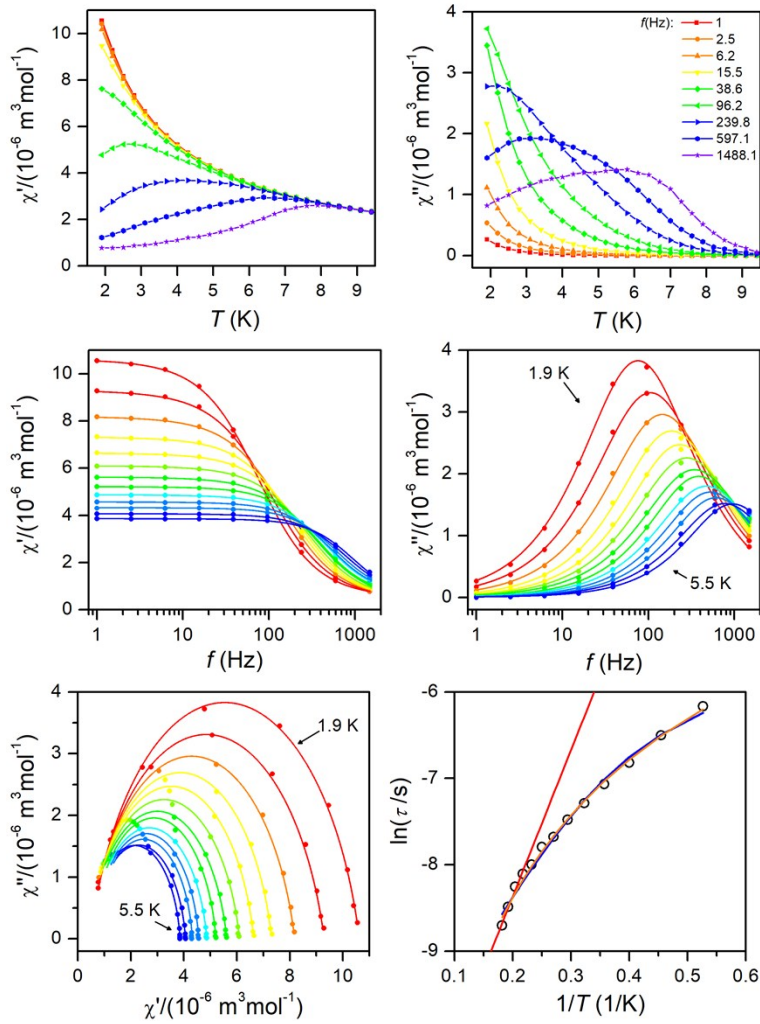
**Figure S14.** In-phase  $\chi_{\text{real}}$  and out-of-phase  $\chi_{\text{imag}}$  molar susceptibilities for **3**. The lines serve as guides for the eyes.



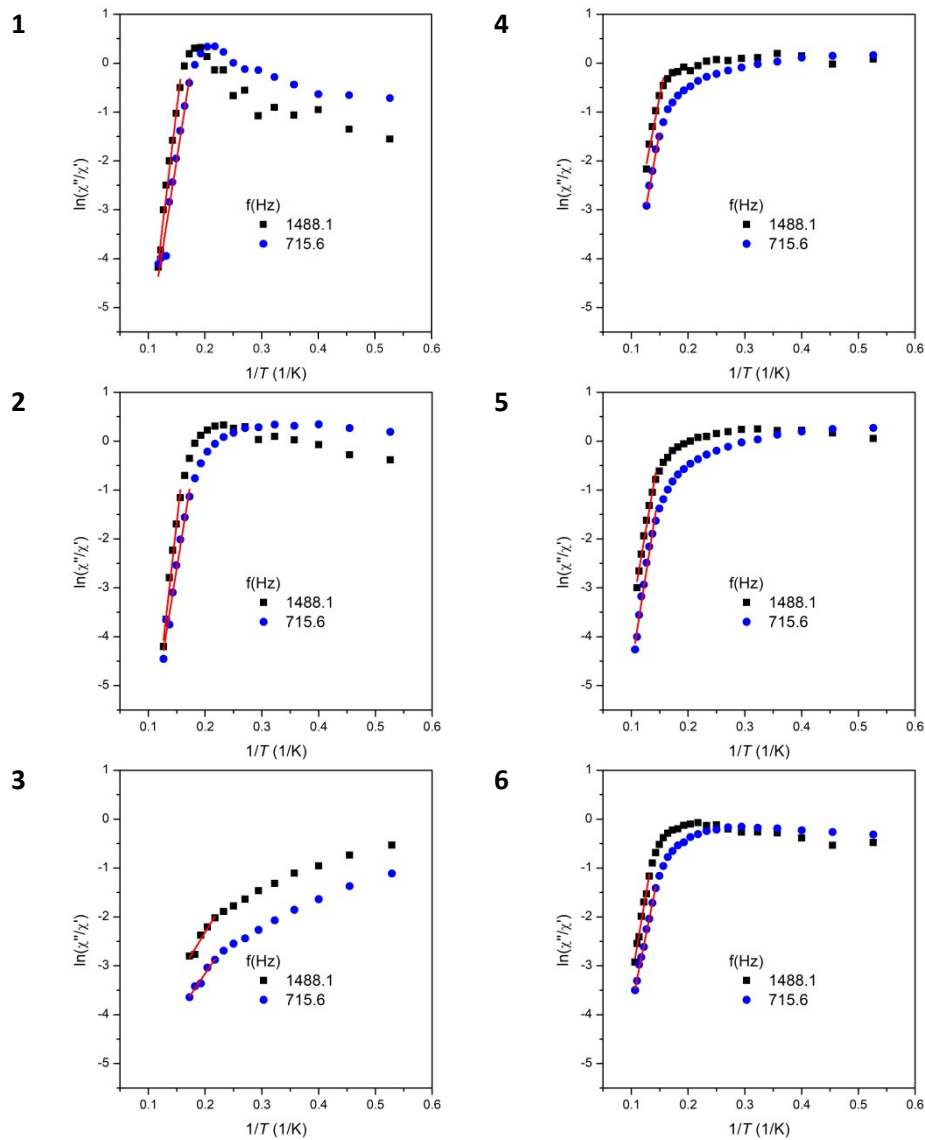
**Figure S15.** AC susceptibility data for **2**. *Top*: in-phase  $\chi'$  and out-of-phase  $\chi''$  molar susceptibilities at the applied external magnetic field  $B_{\text{DC}} = 0.1$  T (full lines are only guides for eyes). *Middle*: frequency dependence of in-phase  $\chi'$  and out-of-phase  $\chi''$  molar susceptibilities fitted with one-component Debye's model using eq. 6 (full lines). *Bottom*: the Argand (Cole-Cole) plot with full lines fitted with eq. 6 and on the left the fit of resulting relaxation times  $\tau$  with Arrhenius law (red line), with the combination of direct and Orbach processes (blue line) using eq. 7 and with the combination of direct and Raman processes (orange line) using eq. 8.



**Figure S16.** AC susceptibility data for **4**. *Top*: in-phase  $\chi'$  and out-of-phase  $\chi''$  molar susceptibilities at the applied external magnetic field  $B_{\text{DC}} = 0.1$  T (full lines are only guides for eyes). *Middle*: frequency dependence of in-phase  $\chi'$  and out-of-phase  $\chi''$  molar susceptibilities fitted with one-component Debye's model using eq. 6 (full lines). *Bottom*: the Argand (Cole-Cole) plot with full lines fitted with eq. 6 and on the left the fit of resulting relaxation times  $\tau$  with Arrhenius law (red line), with the combination of direct and Orbach processes (blue line) using eq. 7 and with the combination of direct and Raman processes (orange line) using eq. 8.



**Figure S17.** AC susceptibility data for **5**. *Top*: in-phase  $\chi'$  and out-of-phase  $\chi''$  molar susceptibilities at the applied external magnetic field  $B_{\text{DC}} = 0.1$  T (full lines are only guides for eyes). *Middle*: frequency dependence of in-phase  $\chi'$  and out-of-phase  $\chi''$  molar susceptibilities fitted with one-component Debye's model using eq. 6 (full lines). *Bottom*: the Argand (Cole-Cole) plot with full lines fitted with eq. 6 and on the left the fit of resulting relaxation times  $\tau$  with Arrhenius law (red line), with the combination of direct and Orbach processes (blue line) using eq. 7 and with the combination of direct and Raman processes (orange line) using eq. 8.



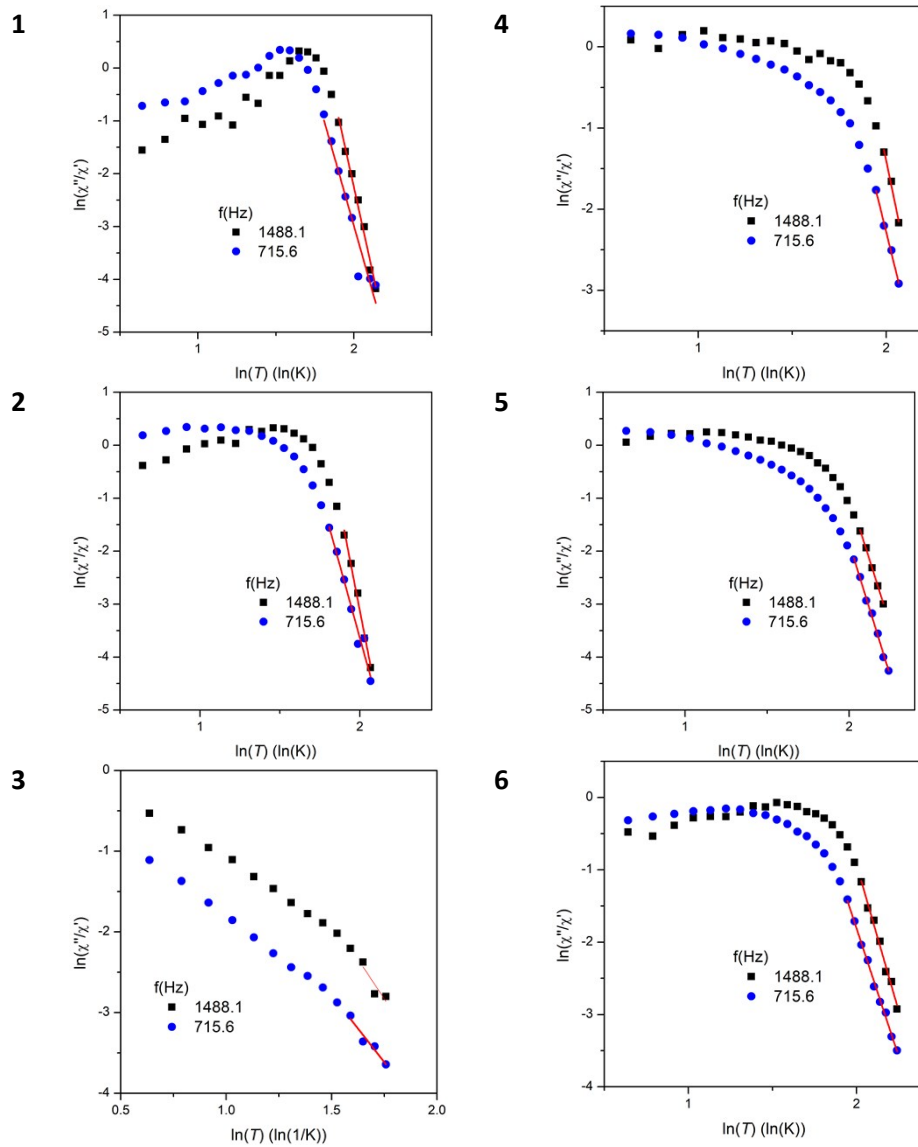


**Figure S19.** Analysis of in-phase  $\chi'$  and out-of-phase  $\chi''$  molar susceptibilities for **1-6** measured at the applied external field  $B_{\text{dc}} = 0.1$  T according to eq. 10. Full points – experimental data, full lines – calculated data.